A&A manuscript no.
(will be inserted by hand later)

Your thesaurus codes are:
04(08.03.1; 08.03.4; 08.09.2: IRC +10 216; 08.13.2; 08.16.4; 13.18.5)

ASTRONOMY
AND
ASTROPHYSICS
18.3.1997

The extended 1.3 mm continuum emission around CW Leo

M. A. T. Groenewegen[1], W. E. C. J. van der Veen[2], B. Lefloch[3], and A. Omont[4]

[1] Max-Planck Institut für Astrophysik, Karl-Schwarzschild-Straße 1, D-85740 Garching, Germany
[2] Department of Astronomy, Columbia University, 538 West 120th Street, New York, NY 10027, U.S.A.
[3] IRAM, Avda. Divina Pastora 7, Nucleo Central, E-18012 Granada, Spain
[4] Institut d'Astrophysique de Paris, CNRS, 98bis Boulevard Arago, F-75014 Paris, France

received, accepted

Abstract. We have obtained a 150 × 150″ map of the 1.3 mm emission around the carbon star CW Leo. Emission is detected at the 3σ level out to a distance of 50″ from the central star. From model calculations we find that the dust density distribution is described by an approximate r^{-2} law superposed on which are possible density enhancements at about 5 and 20″ distance from the star. This could imply phases of enhanced mass loss lasting up to several hundred years duration over the last few 1000 years. The major uncertainty in a quantitative analysis is in the contribution of molecular lines. The density enhancement at 5″ is consistent with a recent phase of increased mass loss as inferred from CO data.

Key words: stars: carbon – circumstellar matter – stars: CW Leo – stars: mass loss – stars: AGB – radio continuum: stars

1. Introduction

CW Leo (= IRC +10 216 = AFGL 1381) is the best studied carbon star because it is intrinsically bright, nearby and has a large mass loss rate. Numerous papers are devoted to the study of the dust emission (see Groenewegen 1997, for a recent study and references to earlier work) and molecular emission (e.g. Guélin et al. 1996, Dayal & Bieging 1995).

Millimetre observations are ideal to study the extended dust envelope as the emission is optically thin and directly traces the density distribution. Contrary to molecular line observations no far-infrared or (sub-) mm maps exist of the dust emission around CW Leo. Continuum observations carried out so far in this wavelength region have been limited to on-source and a few off-source positions using single-channel photometers (Walmsley et al. 1991, Marshall et al. 1992, Althenoff et al. 1994, van der Veen et al. 1995). Here we present the first map of the extended continuum emission surrounding CW Leo.

2. Observations

The data were taken on March 20-21, 1996, with the IRAM 30m dish at Pico Veleta, Spain. We used the MPIfR 19-channel bolometer. The pixels of the array are located at the center and on the sides of two concentric hexagons. Two adjacent channels are separated by 20″, and have a beam width of 11″ FWHM. The different channels have similar sensitivities, apart from channel 11 whose data were discarded. The filter bandpass is between 220 and 280 GHz with an effective frequency of 243 GHz.

On-the-fly maps of size 260 × 150″ were made centered on CW Leo, using a secondary, chopping at a frequency of 2 Hz and a throw of 45″. The source was scanned in the azimuth direction by moving the telescope at a speed of 4″/sec; subsequent scans were spaced by 4″ in elevation. As the pointing was checked on CW Leo itself before starting each map, there is insignificant pointing jitter of order $\lesssim 2''$ between the maps. The FHWM beam size in the final map is therefore 11″. Absolute calibration was done on Uranus. The flux of Uranus at 243 GHz was estimated from the program "Planets" in use at Pico Veleta. The weather was relatively poor. The zenith optical depth was monitored regularly by performing sky dips in the source direction: it was found to vary between 0.25 and 0.40 (corresponding to 3-5 mm of water vapour above the telescope). We used the NIC software developed by IRAM to reduce the data and create the single-beam maps.

Ten maps with a total integration time of 7 hours were co-added to produce the final map, which is shown in Fig. 1. The on-source flux is 1520 mJy. Walmsley et al. (1991) reported four on-source measurements made with the IRAM telescope, with fluxes of 1500, 2550, 1508 and 1466 mJy, during four sessions. For many bright sources the fluxes obtained during their second session were systematically higher. If we were allowed to discard the value of 2550 mJy, then our measured on-source flux determination is in good agreement with their other determinations.

As can be seen from Fig. 1 , the dust envelope was detected at a three sigma level or better out to 50″. Although the inner part of the map looks nicely round (with a slight extension in the North-South direction), the 3 and 4σ contour levels look jagged. It is not clear whether we are affected by noise, or if this is real. The dynamical time scale to reach 50″ is about 2200 years (for a distance of 135 pc, and an expansion velocity of 15 km s^{-1}). If real, and if we assume that CW Leo has been on the AGB for more than 2200 years, this would imply inhomogeneities in the ejected AGB wind.

Send offprint requests to: Martin Groenewegen

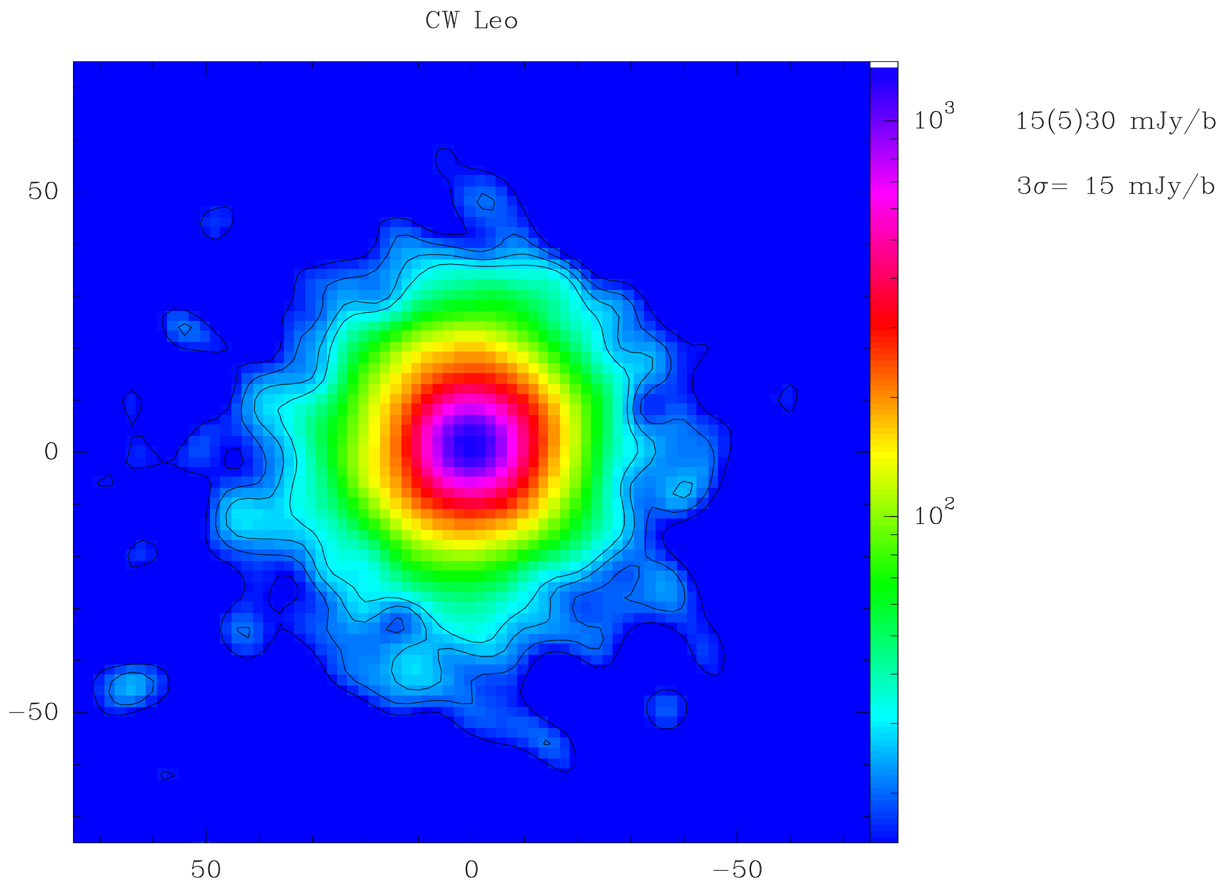

Fig. 1. The 1.3 mm continuum map of CW Leo. The noise level is 5 mJy/beam, and contours are drawn at the 3, 4, 5 and 6 σ level. The map size is 150 × 150″, with north up and east to the left. Scale is in arcseconds.

To determine the flux as function of projected radius we first divided the map in four quadrants and co-added the emission in each quadrant. We found similar results in all four quadrants within the measurement errors. We then co-added the emission over a 360 degree angle to obtain the flux as function of projected radius. This is shown in Fig. 2. The error bars indicate the one sigma variation (in one beam) at a given projected radius over a 360 degree angle.

3. Modeling

We used the optically thin dust model by van der Veen et al. (1994, 1995) to fit the dust emission (i.e., observed flux corrected for photospheric and molecular line emission in the bandpass, as discussed below) as function of projected radius. Instead of fixing the density distribution with a power law we determined the density at various radii in the shell. We assume the following parameters: ratio of absorption coefficient to grain size of $Q(1.3mm)/a = 4.8$ cm^{-1}, specific density of the grains of 2 g cm^{-3}, distance of 135 pc, luminosity of 1.5 $\times 10^4$ L$_\odot$, a stellar temperature of 2000 K, an inner dust radius of 4.47 R$_\odot$, a constant expansion velocity of 15 km s^{-1}, and a gas-to-dust ratio of 200 (see Groenewegen 1997). The model was convolved with a Gaussian 11″ FWHM beam.

It has been recognised that the contribution of molecular lines in the 1300 μm bandpass is not negligible. Estimates for the IRAM 11" beam centered on-source range from 25 or 30% of the observed broad band flux (Walmsley et al. 1991 and Groesbeek et al. 1994 respectively) to 75% at maximum light (Groenewegen 1997). The large range of values as well as the fact that our passband differs slighlty from the ones used in the references above lead us to reinvestigate the contribution of these molecular lines in some detail. We consider the following lines as the main contributors: ^{12}CO(2-1), ^{13}CO(2-1), SiO(6-5), CS(5-4) (Walmsley et al. 1991), H^{13}CN(3-2), SiS(13-12), SiS(14-13) (Groesbeek et al. 1994), HCN(3-2) and SiS(15-14). Because of our different passband SiO(5-4) (Walmsley et al.) and SIS(12-11) (Groesbeek et al.) do not contribute but we have to add HCN(3-2) and SiS(15-14). First we will estimate the on-source line contributions and then we will determine how this contribution changes with projected radius. All integrated intensities below are on a $T_{\rm A}^*$ scale.

Observations by Groenewegen et al. (1996) yield on-source integrated intensities in the 11″ IRAM beam of 461 K km s^{-1} for ^{12}CO(2-1) and 67 K km s^{-1} for ^{13}CO(2-1). For HCN there are no IRAM data, so we used JCMT observations by Williams & White (1992). We first used the model of Groenewegen et al. (1994) to calculate the HCN(3-2) and H^{13}CN(3-2) emission in JCMT beam using a HCN abundance of 8 $\times$ 10^{-6} (Miller & Herbst 1994) and a ratio HCN/H^{13}CN of 44 (Kahane et al. 1992). The results were compared with the values observed by Williams & White and from this we determined scaling factors. Subsequently, the HCN(3-2) and H^{13}CN(3-2) emission

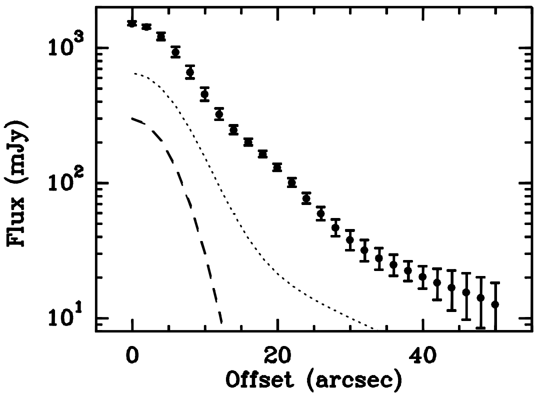

Fig. 2. Observed flux (not beam deconvolved), represented as dots with error bars, photospheric emission (dashed line), estimated molecular line emission (dotted line) (without taking into account molecules distributed in hollow shells).

was calculated in the IRAM beam and the scaling factors were applied. This procedure yields on-source integrated intensities of 833 K km s^{-1} for HCN(3-2) and 521 K km s^{-1} for H^{13}CN(3-2). For the CS(5-4) line Bujarrabal et al. (1994) find an on-source integrated intensity in the IRAM beam of 150 K km s^{-1}. To find the contribution of the SiO(6-5) line we use Walmsley at al. (1991) who reports an on-source combined integrated intensity in the IRAM beam for SiO(5-4), SiO(6-5), ^{12}CO(2-1), ^{13}CO(2-1) and CS(5-4) of 1105 K km s^{-1}. Given the numbers we found earlier for CO and CS this leaves 427 K km s^{-1} for the two SiO lines. We estimate the 6-5 line to contribute 15% of that, or 64 K km s^{-1}. Sahai (1984) observed several SiS lines with a 4.9m telescope. We assume that the intensities with IRAM are a factor of (15/4.9)^2 larger. For the J=13-12, 14-13 and 15-14 lines we then find a total intensity of 770 K km s^{-1}. Walmsley et al. estimate all weaker lines to contribute 1080 K km s^{-1}. This yields a grand total for the on-source molecular line contribution of 3946 K km s^{-1}. Using the conversion from $T_{\rm A}^*$ to Jansky at these frequencies of 12 Jy/K (IRAM Newsletter) and the fact that 60 GHz passband corresponds to a velocity of 72 500 km s^{-1}we find an on-source contribution of molecular lines in our passband of 0.65 Jy.

The radial dependence of the molecular line emission is explicitly calculated for CO and HCN by using the results from model calculations by Groenewegen et al. (1997a) who modeled the ^{12}CO and ^{13}CO J=1-0 up to J=6-5 observations of CW Leo. Using a distance of 135 pc we took the best fitting model from Groenewegen et al. (1997a) to determine the intensity of the CO lines in the IRAM 11$''$ beam as a function of radial offset. HCN was included in the model using a 1/e-radius of the HCN abundance of 14$''$. For the SiS lines we assumed a 1/e-radius identical to HCN as a compromise between earlier findings of Sahai (1984) who found 22$''$ and Bieging & Tafalla (1993) who found 8$''$. For CS, SiO and the weaker lines we also assume the same radial dependence as for HCN, the argument being that we expect most molecules to be photodissocated at similar distances from the star.

We attempted to make the most accurate estimate of the contribution of the molecular lines as explained above. The result is the dotted line in Fig. 2. It should be recognised however that there still may be substantial errors. Firstly, there is the absolute callibration of the line observations, which typically is 30%. The other is the radial dependence, in particular of less known species.

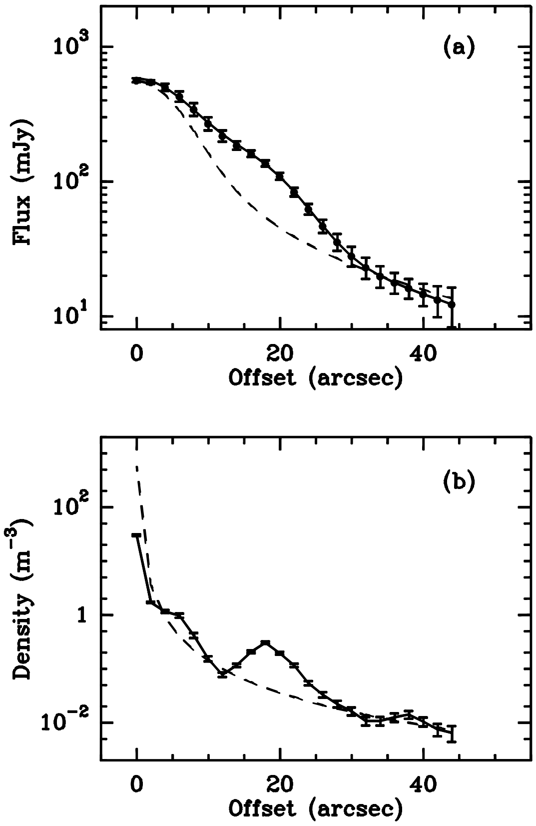

Fig. 3. a) Dust emission as function of projected radius. The full curve shows the result of the best fit to the data points (the solid dots) for the density profile shown as the full line in panel (b). One sigma errorbars are indicated. The dashed curve shows the result assuming steady mass loss. **b)** Density profiles corresponding to a steady mass loss (dashed curve) and the best fit (full curve) respectively. In both figures the extended emission of molecules distributed in hollow shells is not taken into account.

The density profile was fitted using an iterative technique which after 30 iterations converged to the solution shown by the full curve in Fig. 3b. The resulting fit to the dust emission including 1σ errorbars is shown in Fig. 3a. For comparison we also show the emission resulting from a $1/r^2$ density law corresponding to steady mass loss fitted through the innermost data point as indicated by the dashed curve in Fig. 3a.

4. Discussion and conclusions

The observations are clearly not in agreement with steady mass loss. There are two well defined enhancements in the density distribution compared to steady mass loss, one between 2 and 8$''$ and a second one between 10 and 25$''$. There may be a third small density enhancement around 38$''$. To verify that these density enhancements are no artifact caused by subtracting the molecular line contributions, we also fitted the data while neglecting the contributions of the lines. We found a result similar to the one shown in Fig. 3 with density enhancements in the same places.

However, it is known that many molecules, formed by photosynthesis in the outer layers of the envelope, are distributed in hollow shells with radius typically $\sim 15''$ (see e.g. Fig. 3 of Guelin et al. 1996). This is in the range where the difference between the two curves of Fig. 3a is largest. We have tried to make a rough estimate of the excess of emission at $\sim 15''$ of the molecules distributed in such a way. This is not easy since we are not aware of good quality maps for most of the corresponding lines in our 1.3 mm bandpass. We based our analysis mostly on unpublished maps with the IRAM 30m of C_4H(23-22), SiCC($9_{27}-8_{26}$) and CN(2-1) kindly provided by C. Kahane and the map of $C_4H(\nu_7)$ of Audinos et al. (1994), to estimate the total contribution of these species. Then we inferred the contribution of C_2H(3-2) and of HNC(3-2), and finally made a guess for the contribution of the other weaker lines. With contributions of the same order of magnitude for these three groups of lines, we derive a total excess of about 60 mJy at $15''$ with respect to the molecular contribution of Fig. 2, with a large uncertainty which could reach 50%. This is to be compared to the difference between the two curves of Fig. 3a, $\sim$100 mJy. It is thus not completely excluded, although somewhat unlikely, that the total excess at 15" is explained by such extended molecular emission. However, from the map of Fig. 3 of Guelin et al. (1996), it does not seem that such 1.3 mm emission of all molecules, except CN, could significantly extend beyond $20''$, and thus explain the excess observed there in Fig. 3a. In conclusion, the extended molecular emission of such molecules accounts probably for a significant fraction of the excess at distances $< 15''$, but probably not for the totality, especially beyond 20". Therefore, the observations seem incompatible with steady mass loss.

Assuming the above quoted distance and expansion velocity through the shell, the variations in the density profile (Fig. 3b) could correspond to changes in the mass loss rate by factors of two to seven, at two epochs in its recent mass loss history: 200 and 850 years ago, of 250 and 600 years duration, respectively.

Sahai (1987) and Truong-Bach (1991) presented evidence for a higher mass loss rate in the past based on CO molecular line emission. Both find approximately a factor of 2 difference over a region of about $5''$. This would be consistent with the first enhancement seen in the dust map between 2 and $8''$.

If the density enhancements are real, the associated time scales are difficult to put in the framework of AGB evolution as we know it. The time scales of hundreds of years are much too long to be related to pulsation, and much too short to be related to thermal pulses.

The luminosity of 15,000 $L_\odot$ assumed for CW Leo is based on a new period-luminosity relation (Groenewegen & Whitelock 1996). Using the core mass-luminosity relation of Wagenhuber (1996), this implies a core mass of 0.76 $M_\odot$, assuming solar metallicity, that CW Leo is in a phase of quiescent hydrogen burning, undergoes no hot bottom burning, and has experienced sufficient thermal pulses so that so called "turn-on effects" are not important. Under the same assumptions the interpulse time between two consecutive thermal pulses is then 18,000 years. The duration of the phases of high mass loss implied by our observations corresponds therefore to typically 1% of the interpulse time. The new AGB evolutionary models of Wagenhuber (1996) do not predict such secular variations in the time evolution of the luminosity in stars with core masses as high as inferred for CW Leo.

We can only speculate about the cause of the possible density enhancements. Recently, Osterbart et al. (1997) presented a diffraction-limited speckle-masking observation of CW Leo at a resolution of $0.092''$. Their image shows a resolved central peak surrounded by patchy circumstellar matter. The brightest clump is 0.13-0.21$''$ separated from the central star at a position angle of about 20^0. The peak emission of this clump is about 40% of that of the central star. Osterbart et al. speculate that the mass outflow is stochastic, and may be caused by shock waves induced by pulsation.

A change in the behaviour of the central star and the immediate consequence this has on the dust formation process is a plausible explanation for the density enhancements. There is a good correlation between mass loss and pulsation period for Miras, in the sense that higher mass loss rates are associated with longer periods (e.g. Whitelock et al. 1994 for O-rich Miras and Groenewegen et al. 1997b for carbon Miras). May be CW Leo changed pulsation mode (for unknown reason) from first overtone to fundamental mode pulsation (and back again after a few hundred years). This would lead to a longer period for a given radius and mass, and this would most certainly have an effect on the circumstellar shell.

References

Althenoff W.J., Thum C., Wendker H.J., 1994, A&A 281, 161
Audinos P., Kahane C., Lucas R., 1994, A&A 287, L5
Bieging J.H., Tafalla M., 1993, AJ 105, 576
Bujarrabal V., Fuente A., Omont A., 1994, A&A 285, 247
Dayal A., Bieging J.H., 1995, ApJ 439, 996
Groenewegen M.A.T., 1994, A&A 290, 531
Groenewegen M.A.T., 1997, A&A 317, 503
Groenewegen M.A.T., van der Veen W.E.C.J., et al., 1997a, in prep.
Groenewegen M.A.T., Whitelock P.A., 1996, MNRAS 281, 1347
Groenewegen M.A.T., Whitelock P.A., Smith C.H., Kerschbaum F., 1997b, MNRAS, submitted
Guélin M., Lucas R., Neri R., 1996, in: "Science with large millimetre arrays", Ed. P. Shaver, Springer Verlag, p. 276
Kahane C., Cernicharo J., Gomez-Gonzalez J., Guélin M., 1992, A&A 256, 235
Marshall C.R., Leahy D.A., Kwok S., 1992, PASP, 104, 397
Miller T.J., Herbst E., 1994, A&A 288, 561
Osterbart R., Balega Y.Y., Weigelt G., Langer N., 1997, in: "IAU symposium 180 on Planetary Nebulae", in press
Sahai R., 1984, ApJ 284, 144
Sahai R., 1987, ApJ 318, 809
Truong-Bach, Morris D., Nguyen-Q-Rieu, 1991, A&A 249, 435
van der Veen W.E.C.J., Waters, L.B.F.M., Trams, N.R., Matthews, H.E., 1994, A&A 285, 551
van der Veen W.E.C.J., Omont A., Habing H.J., Matthews H.E., 1995, A&A 295, 445
Wagenhuber J., 1996, Ph.D. thesis, Technische Universität München
Walmsley C.M., et al., 1991, A&A 248, 555
Whitelock P.A., et al., 1994, MNRAS 267, 711
Williams P.G., White G.J., 1992, A&A 266, 365